# Optimized Fuzzy and Neuro-fuzzy Controller based MPPT using MOHGA applied for a Solar Photovoltaic Module

RATI WONGSATHAN
Department of Electrical Engineering, Faculty of Engineering
North-Chiang Mai University
169 Hangdong Chiang Mai, THAILAND 50230 Tel.+66(53)819999, Fax. +66(53)819998
rati1003@gmail.com, rati@northcm.ac.th

*Abstract:-* Maximum power point tracking (MPPT) is a significant technique in order to handle the maximum power utilization of the photovoltaic regulator. By this technique, the operated voltage is perturbed from the closed-loop control algorithm untill reaching the MPP by changing the duty cycle ratio of the DC-DC converter ciucuit. To achieve this power management, this paper integrated offline genetic algorithm (GA) with fuzzy logic (FL) and neuro-fuzzy (NF) to proposed FL controller (FLC-GA) and NF controller (NFC-GA). A Multi-Objective Hierarchical GA (MOHGA) is applied to select the control rules silmutaneously to fine the tuned system parameters. Furthermore, the intentional aim of this paper is to find a minimum set of fuzzy rule that can achieve the MPP with acceptable accuracy. Conseqently, the optimized FLC-GA and optimized NFC-GA are alternately proposed to optimize the complexity of the FLC-GA and NFC-GA in order to avoid the over-fitting computation which may lead to miss the MPP. The measured voltage and current are directly computed the slope of *P-V* curve and its change to set as the inputs of the controller while the duty cycle ratio is generated for the controlled output at the given various change weather conditions. Unlike focusing only on the change of the irradiance effect, in this work the panel temperature changing is together considered especially for the case of low irradiance and high temperature. Fast risetime response at the transient state and the stabilzed accuracy at the steady state are used as the controlled performance assesments. In order to prove the effectiveness of the proposed hybrid controllers, the simulations are tested before the practically implementation by using Matlab/Simulink. From the simulation results, the FLC-GA dominantly performs the best stabilized accuracy compared to the optimized NFC-GA, the NFC-GA, the optimized FLC, the conventional FLC, the IC method and the P&O method respectively. In the case of the rise time, the optimized NFC-GA dominantly performs the fastest tracking to the MPP than the NFC-GA, the optimized FLC-GA, the conventional FLC, the FLC-GA, the P&O method, and the IC method respectively. Trading off between the fast time response and stabilized accuracy, the optimized NFC-GA performs most the best.

*Key-Words:* - Optimized Fuzzy logic control, Optimized Neuro-fuzzy control, Multi-objective hierarchical genetic algorithm, and MPPT.

## 1 Introduction

Nowadays, the renewable energy source is investigated and developed over worldwide since the lack of natural fuel source such as coal, natural gas, petroleum, etc. in the nearly future and rapidly increasing of the environmental degradation. According to the information of International Renewable Engergy Agency or IRENA in 2015, the most renewable power capacity are wind power and solar energy. Solar or photovoltaic (PV) energy, which is economical source of energy becomes a promising alternative since it is free and abundant in most part of the world [1]. It is also clean which produce neither the green house effect gas nor toxic waste through its utilization. In addition low running and maintenace cost and also noiseless operation due to absence of moving part are the avantages of PV system. Considering for the growing demand of electricity for domestic comsumption in ASEAN countries, it is expected to more than double in the next 25 years, 2040 [2]. Therefore, the demand of PV generation systems seem to be simultaneously increasing for both standalone and grid-connected modes of PV system since almost all countries in these nations are located near the equator which will get most high irradiance throughout the year. However, the electricity generated from PV system remains significantly more expensive than the conventional sources due to the low efficiency of conversion energy by the commercial PV(only 9 to 16%), especially under low irradiance conditions [3]. The electrical power generated by PV also changes continuously with the environmental

conditions mainly the irradiance (*G*) and ambient temperature (*T*) which are another disadvantages. To obtain the maximum efficiency of the PV, it is necessary to operate the PV at its maximum power point (MPP) for all environmental conditions. To overcome this problem, the maximum power point tracking (MPPT) technique will be developed and applied in the PV power system. The efficiency of MPPT depends on both MPPT control algorithm and the MPPT circuit. The MPPT control algorithm is usually applied in the DC-DC boost converter which is normally interfaced between PV panel and load. The operating point is converged to the MPP by varying the duty-cycle of the power converter through the control command from the pulse width modulation (PWM) signal. The typical diagram of power control based MPPT of the PV system with the swithching interface is shown in Fig.1.

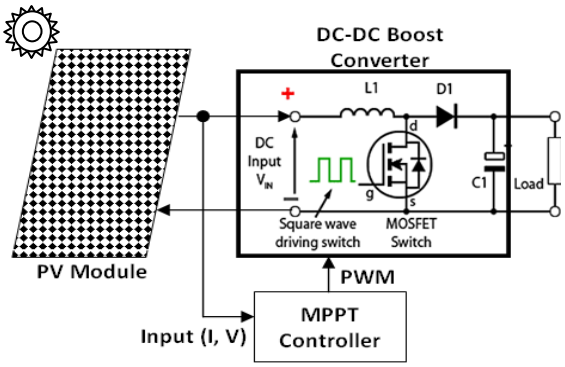


Figure1. Typical diagram of power control based MPPT of PV system.

Extracting the maximum power output from the PV panel which is available only at one spectific condition, a number of control algorithms based on MPPT are developed in the various ways. MPPT technique can be divided into 2 main groups: dynamic and static methods. Dynamic method is based on tracking the sun movement by using additional mechanical engine with a high cost and high energy consumption while the static method applied the high frequency power converter of electronic device to continuously adjust the operating point to the MPP [4]. The static MPPT technique which is more interesting can be broadly classified into three topologies including perturb & observe methods (P&O) and its modified, the incremental conductance methods (IC) and its modified, and the aritificial intelligence (AI) based methods such as neural networks (NNs), fuzzy logic (FL) and the hybrid neuro-fuzzy (NF) which were represented in literature [5]-[9]. In the literatures, P&O and IC methods operates well for the slowly change of weather condition but it presents the slow response speed and even tracking in wrong direction way under rapidly change of weather condition. Although, they take an advantage in practical implementation and simple methodology, they always suffer from large power oscillation which is poorly stable and accuracy at the transient state due to the highly non-linear nature and time varying of the PV characteristic. In order to automatically adjust the control step sizes to keep up with the change of weather condition, the variable step sizing algorithms which is based on adaptive and AI techniques are the best choice.

AI based methods are increasingly popular adopted in MPPT due to the learning property in interpolation and extrapolation of the non-linear nature of any data with high accuracy. NNs is a powerful technique for leaning the relationship of input-output data but it lacks the heuristic sense and works as a black box [10]. Some of applications of NNs based MPPT in PV are presented in [11]-[13]. This method is not suitable in the real parctice because it requires a large number of weather conditions data in order to train the networks. Especially In the case of PV array, the input of the NNs controller which consists of *G* and *T* cannot be implemented because of the different characteristics of each module in the array. Moreover, the extra cost and the sensivity of irradiance and temperature sensor are also considered in the household standalone implementation. On the other hand, FL control (FLC) is implemented without requiring such the big data and sensor. It has the capability of mapping heuristic and linguistic terms of the unknown system into numerical values through the designed fuzzy rules and membership function. It also returns the heuristic output by quantifying the actual numerical data into heuristic and linguistic term [14]. The FLC based MPPT for PV sytem is available in [15]-[16] which have high tracking accuacy under steady state of weather condition but still exhibits some trade-offs between tracking speed and tracking accuracy at the fast change weather condition. Although, it has some advantages of being robust, design simplicity, and minimal requirement for accurate mathematical model. The difficult of parameter selection of the membership functions and fuzzy rules is the main criteria which directly rely on the prior knowledge of the system. Recently, it integrates the potential benefits of NNs and FL to form a hybrid system as ANFIS architecture in order to estimate the MPP which is utilized in [17]-[20].

In general, ANFIS based MPPT found in the literatures can be divided into 2 groups depending on the inputs of the ANFIS controller. The first group had directly taken the voltage and current information from the PV pannel as the input while the second group had utilized the weather information such as *G*, *T*, and etc to estimate the MPP and then uses the output as the reference input for another controller. However, a large number of collected data from several experiments performed in various weather condition are practically inappropriate. Temperature sensing is simple but solar irradiance measuring is difficult since irradiance sensors are high cost and tedious task to calibrate. Futhermore, the error between the estimated MPP from ANFIS and instant power and also overshoot are needed to be eliminated by the others controller such as PI or fuzzy controller as another drawback. Althoug FLC and NFC based MPPT provide superior tracking performance, the design for complexity on different kinds of these techniques are significantly realized and considered.

In this work, an increasing of efficiency on energy conversion of solar PV by static MPPT method through the AI approaches including adaptive fuzzy and neuro-fuzzy controller is our main goal. In order to overcome the parameters and rules selection, the optimization technique as multi-objective hierarchical genetic algorithm (MOHGA) has been introduced to generate the optimized FLC-GA and NFC-GA under the rapidly change weather (i.e. *G* and *T*) conditions. To avoid the using of one more controller and without more expensive sensor, generating the direct duty cycle is generated as the output by account for the derivative of power with respect to voltage or current and its variation as the inputs is also considered here. The comparison performance of both transient and steady state for all proposed controllers with the conventional controllers can be a bases in making decision to select the appropriate controller.

The rest of the paper is organized as follows. The overall system configuration including equivalent circuit of PV modeling with its parameters. Secondly, the *I-V* and *P-V* characteristic formaulation and the switching device of the interfacing circuit are detailed in section 2. Thirdly, some various controllers are conceptualized to describe the design in step by step procedure presented in section 3. Next, the structural design of controllers and their controlled results are shown in section 4 with the discussions. Finally, the conclusion is made at the end of the paper in section 5.

# 2 PV System and Interface

In order to facilitate the most appropriate and robust control method for the overall efficiency of PV system, it is necessary to provide a more accurate optimize algorithm to extract an equivalent parameters of PV models prior to its installation. In this work, the implicit function of I-V characteristic of PV module in various weather conditions with *G* and *T* is captured off-line by the neural networks model. The input of the networks combines the output current, voltage and the equivalent electrical parameters. The initial parameters are preliminarily search by GA at the standard test condition (STC) from the measured *I-V* extraction. The initial parameters are mapped to the given weather conditions by using the translation function. The detail of PV modelling including with the electrical characteristic and the PV interface are described in subsections 2.1 and 2.2 respectively.

## 2.1 PV Modeling

PV cell is basically fabricated from a p-n junction in a thin wafer or layer of semiconductors. The electromagnetic radiation of solar energy can be directly converted to electricity through photoelectric effect [21]. A solar module with consisting of the multi solar cells has the same current-voltage (*I-V*) characteristic except with the change in the magnitude of current and voltage. This section exhibits the solar PV module *I-V* characteristic obtained from the simulation by Matlab/Simulink. The convenient and most common way in most simulation of PV model is the single diode lumped equivalent circuit model [22] which is composed of 5 parameters i.e. the photo-current ($I_{pv}$), diode saturation current ($I_{sd}$), series resistance ($R_s$), parallel or shunt resistance ($R_{sh}$), and the ideality factor of diode ($n$) which are shown in Fig. 1. In order to track the MPP of the PV system by the various control techniques, the accuracy of method depends on the knowledge of these PV parameters which are usually extracted from the experimental data. In this work, achieving the utilizable desire voltage level, a number of PV cells are used to form a solar module in connected series. However, there is no more detail about the characteristic of PV module at any weather condition from the factory. For more efficient design on power conversion of PV module including program simulation, the

model of PV module is necessary. In our experiment, a poly-crystalline silicon commercial (SHARP type ND-130T1J) with 36 c ells ($N_s$) in series connected is adopted to extract the PV module parameters under various environment conditions.

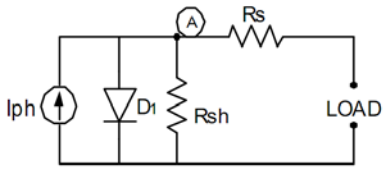


Figure 2. The equivalent circuit with single diode model of the PV module.

An equivalent circuit of PV module which is referenced in Fig. 2 and composed of $N_s$ cells in series connection produces the non-linear load current ($I_L$)-voltage ($V_L$) characteristic and can be expressed as

$$I_L = I_{pv} - I_{sd}\left(\exp\frac{q(V_L/N_S + I_L R_S)}{nK_B T} - 1\right), - \left(\frac{V_L/N_S + I_L R_S}{R_{sh}}\right) \quad (1)$$

where $K_B$ is Boltzmann's constant, $q$ is the electronic charge, and $T$ is the temperature in Kelvin. From eq. (1), the 5 parameters ($I_{pv}$, $I_{sd}$, $R_s$, $R_{sh}$, and $n$) are determined from the *I-V* characteristic which is obtained from the experiment. The measured current and voltage were experimentally done at the STC i.e. 1 k W/m$^2$ of irradiance and 25 °C of temperature. Our proposed GA was applied to extract the preliminary parameters by using this measured current and voltage values. In order to describe the influence of weather conditions on the parameters of a single diode model, the translation method was applied by using the parameter identification and translation formula. The characteristic *I-V* of the PV module at various weather conditions was finally off-line captured by NNs. While the translation parameters and input variable (voltage and current) will be used as the input of NNs to form the PV module characteristic which is illustrated in Fig. 3.

PV module parameters on various weather conditions are then estimated by translation equation (Blaesser et al., 1988; Anderson, 1996; Marion 2002; Hermann et al., 1996; Tsuno et al., 2005). The results were demonstrated through linear variation of short circuit current with $G$ in eq. (2) and variation of open-circuit voltage with $T$ in eq. (3) from condition ($G_1$,$T_1$) to ($G_2$,$T_2$).

$$I_{sc}(G_2,T_2) = I_{sc}(G_1,T_1)\times\frac{G_2}{G_1}\left[1+\alpha(T_2-T_1)\right], \quad (2)$$

$$V_{oc}(G_2,T_2) = V_{oc}(G_1,T_1)\times\left[1+\beta(T_2-T_1)\right]\times\left[1+\delta\ln\left(\frac{G_2}{G_1}\right)\right], \quad (3)$$

where $\alpha$ and $\beta$ are the temperature correction factors, and $\delta$ is the irradiance correction factor. The translation method was applied to eq. (1) and by parameter identification, the translation formulas of five parameters in single diode model can be expressed by eq. (4)-(8),

$$I_{ph}(G_2,T_2) = (G_2/G_1)\times\left[1+\alpha(T_2-T_1)\right]I_{ph}(G_1,T_1) \quad (4)$$

$$I_S(G_2,T_2) = (G_2/G_1)\times\left[1+\alpha(T_2-T_1)\right]I_S(G_1,T_1) \quad (5)$$

$$R_s(G_2,T_2) = \frac{\left[1+\beta(T_2-T_1)\right]\left[1+\delta\ln(G_2/G_1)\right]}{(G_2/G_1)\left[1+\alpha(T_2-T_1)\right]}R_s(G_1,T_1) \quad (6)$$

$$R_{sh}(G_2,T_2) = \frac{\left[1+\beta(T_2-T_1)\right]\left[1+\delta\ln(G_2/G_1)\right]}{(G_2/G_1)\left[1+\alpha(T_2-T_1)\right]}R_{sh}(G_1,T_1) \quad (7)$$

$$n(G_2,T_2) = \frac{q}{K_b T}\left[1+\beta(T_2-T_1)\right]\left[1+\delta\ln(G_2/G_1)\right]n(G_1,T_1) \quad (8)$$

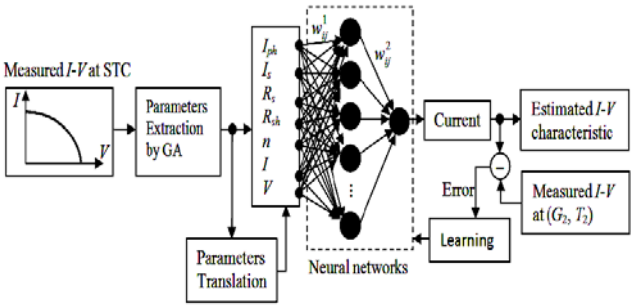


Figure 3. The block diagram of *I-V* characteristic generation of the PV module at the various weather conditions are obtained by the NNs model together with the translation method of initial parameters extraction from GA.

From Fig. 3, t he preliminary parameters extracted by GA method, current and voltage variable simultaneously with parameter translation were preliminarily used as the inputs of the NNs which are in simple 3 layers in the structure i.e. input layer with input nodes, hidden layer with $N$ hidden node and nonlinear function commonly hyperbolic tangent function $g(.)$, and an output layer with linearly transfer function $f(.)$. The output of

NNs ($I_{est}$) is the weighted summation of each hidden layer neuron's output which can be expressed as

$$I_{est} = f\left(b^{(2)} + \sum_{j=1}^{N} w_{j1}^{(2)} \cdot g\left(\sum_{i=1}^{6} w_{ij}^{(1)} PV_i + b_i^{(1)}\right)\right), \quad (9)$$

where $w$ and $b$ is the weight and bias which are searched by the well known back-propagation method.

The initial module parameters extracted from measured I-V characteristic by GA at the STC are found as $I_{ph}$ = 8.01, $I_s$ = 8.77×10$^{-6}$, $R_s$ = 16.1m, $R_{sh}$ = 690.72, and $n$ = 1.73. These parameters are then translated by using translation function with determined correction factor ($\alpha$ = -0.048 °C$^{-1}$, $\beta$ = -0.0194 °C$^{-1}$ and $\delta$ = 0.06) for the various weather conditions $G$ and $T$. The PV module characterized by the hybrid NNs with parameter translation method initiated parameter extraction by GA for various weather conditions are shown in Fig. 4 (a)-(b). In the case of constant temperature in Fig. 4 (a), the irradiance are varied from 1000 to 400 W/m$^2$ by the decreasing step size of 200, whereas the characteristic of *I-V* are simultaneously changed. It is shown that the short circuit current has linear relation with solar irradiance while the open circuit has a non-linear relation. In Fig. 4 (b), while $G$ is kept constant and set to 1000 W/m$^2$, $T$ is varied from 25 to 40 °C by the increasing step size of 5, the short circuit current has slightly changed while the open circuit voltage has linearly varied with temperature. In Fig. 4(c) and (d), a typical characteristic exhibits the varying of power with distinct maximum power for each solar irradiance and temperature respectively. The MPP significantly reduces along with the reduction of solar irradiance and increment with temperature which is the challenge of matching proper load for with PV module. In our simulation from the experimental data, the varying solar irradiance has effect on the maximum available power from PV module similar with the varying temperature. The locus of the MPP shows that the voltage at which existing MPP varies approximately 75.3-83.5% and 16.8-25.0% from the short circuit and open circuit respectively for the varying solar irradiance. While the MPP voltage varies approximately 45.5-79.5% and 20.4-54.5% from the short circuit and open circuit respectively for varying temperature. In the next section, the fuzzy controller consequently utilizes these data to design the membership function and decision rules.

The *I-V* characteristic results are obtained from MATLAB/Simulink before the actual tested without the real weather conditions in order to protect the damage of equipment and for its convenience. The *I-V* characteristic from our simulation results yield well match with the experimental results. The MPPs calculated from the simulated *I-V* characteristeic are used as t he refferences of the controlled outcomes from the proposed controllers in section 4.

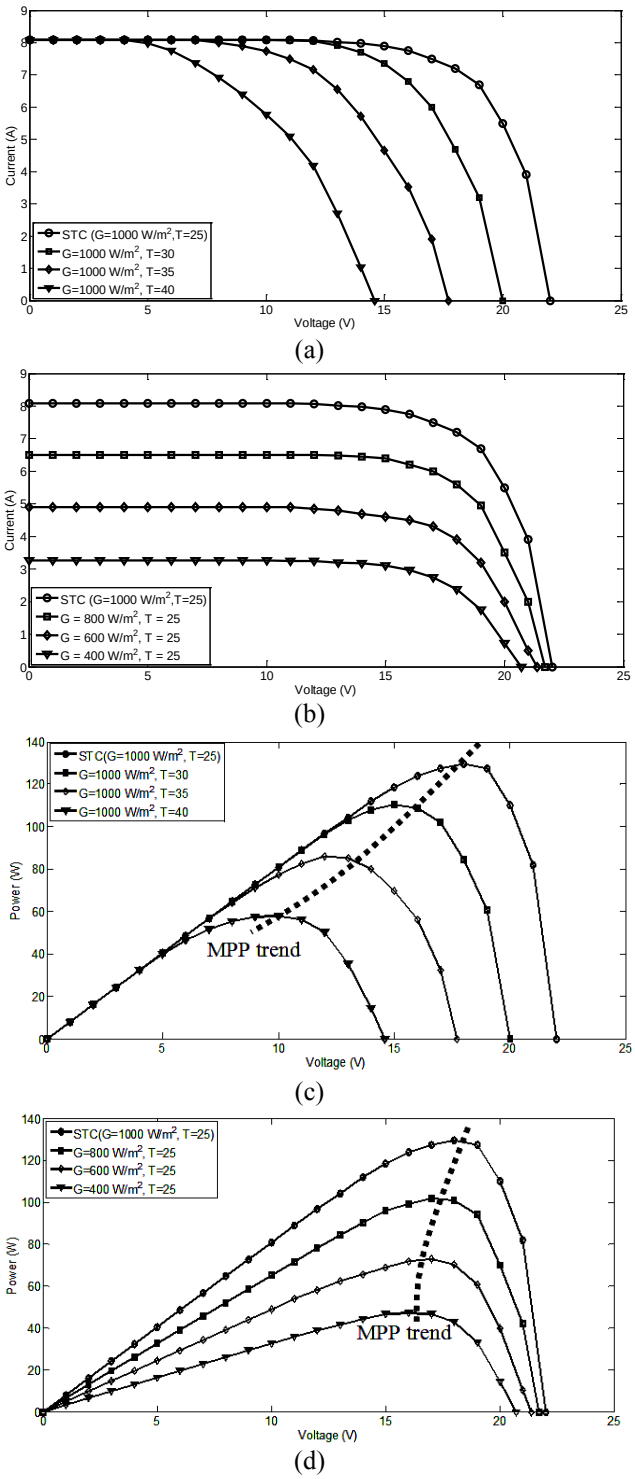


Figure 4. The *I-V* and *P-V* characteristic of the PV module in the case of (a) and (c) varying of the irradiance conditions, and (b) and (d) varying of the temperature conditions.

### 2.2 DC-DC Boost Converter

DC-DC boost converter can be used as switching-mode regulator to convert an unregulated dc from PV to a regulated dc output voltage for the load. Pulse width modulator (PWM) is normally regulated the voltage. While the MOSFET or IGBT is used as t he switching device. The design and implementation of this part of circuit is conventional, therefore it will not be discussed further here. To step up the dc voltage, the DC-DC boost converter is introduced to interface the PV module and the resistive load which was shown in Fig. 1. The MPP is reached when the MPPT algorithm changes and adjusts the duty cycle of the DC-DC boost converter. Through averaging concept, the input-output voltage relationship for continuous conduction model under steady state is here by given

$$\frac{V_o}{V_{in}} = \frac{1}{1-D} \quad (10),$$

where $D$ is duty cycle and varies between 0 a nd 1, thus the output voltage must be higher than the input voltage in magnitude. Similary, the relationship between input impedance ($R_{in}$) and load impedance ($R_{Load}$) of a boost converter can be expressed as

$$R_{in} = (1-D)^2 R_{Load} \quad (11).$$

From eq. (11), it's quite clear that by varying the duty cycle, the input resistance can easily be changed. The increasing duty cycle resulted the decrease of input impedance, the operation point is moved to the intersection of the load line number 2 and *I-V* curve in Fig. 5. In contrary, the operation point moves to the intersection of the load line number 3 and *I-V* curve. Untill duty cycle converges to the optimal, the operation point achieves the MPP at the intersection of load line number 1 a nd *I-V* curve.

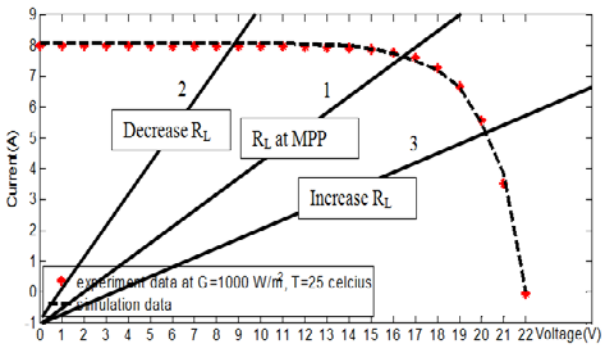


Figure 5. The transition of the operating point location dues to the variation of load impedance.

After filtering the required data from the PV panal ($V$ and $I$) through A/D module, our differently implemented controller based MPPT schems will perform to provide the PWM signal for the boost converter in order to generating the controlled duty ratio. The detailed descritption of these controllers will be discussed in the next section.

## 3 Controller based Static MPPT Technique

In this paper, the controlled performance of our proposed fuzzy logic control (FLC) and neuro-fuzzy controller (NFC) are implemented together with the widely and simple used MPPT techniques i.e Perturb & Observe (P&O) and Incremental Conductance (IC) method. The detailed concept and stewise procedure including of P&O and IC, FLC, FLC-GA and optimized FLC-GA, NFC-GA and optimized NFC-GA method are described in the sub-section 3.1-3.5 respectively.

### 3.1 Perturb & Observe (P&O) and Incremental Conductance (IC) Method based MPPT

The conventional and popular P&O algorithm with fixed step duty cycle method is the simplest algorithm and easiest way to implement as compared to other methods [23]. In this technique the power $P_1$ corresponds with the instantly measured voltage ($V$) and current ($I$) from PV panel is firstly computed to observe the power $P_2$ after perturbation of a small voltage ($\Delta V$) or duty cycle ($\Delta d$) to the dc/dc converter in one specific direction. By the comparing, if $P_2$ is more than $P_1$ then the perturbation is in the right direction. Otherwise, the reverse direction is repeatedly done untill it met the MPP ($P_{mpp}$) and also corresponding MPP voltage ($V_{mpp}$). However, it does not work well with the rapidly change of the weather condition due to its fixed a nd small step size of $\Delta D$. It cannot stop at the MPP but fluctuates around or near the MPP at the steady state. Then the proper perturbation size is a significantly criteria in providing good performance for both transient and steady-state response. The disadvantages of these method are concurrently seen with the experimental results in the next section 4.1.

To improve the lack of controlled response efficiency from P&O based MPPT under fast varying weather conditions, the incremental

conductance or IC method [24] is intoduced. This method always adjusts the output voltage according to the MPP voltage based on the incremental and instantaneous conductance ($G$) of PV module [25]. It exploits the assumption of the ratio of change in output conductance is equal to the negative output conductance at the MPP ($\partial P/\partial V = 0$ while $\partial P/\partial V < 0$ and $\partial P/\partial V > 0$ means the operating point is to the right and left of MPP respectively) or

$$\Delta G = \frac{\Delta I}{\Delta V} = -\frac{I}{V} \quad (12).$$

If this condition is not met that means $\Delta I/\Delta V > -I/V$ (operating point at the left of MPP) or otherwise, the direction at this operating point must be perturbed until the relationship in eq. (12) succeeds. Thus, MPP can be tracked by comparing the instantaneous conductance ($I/V$) to the incremental conductance ($\Delta G$). It can be determine that the MPPT has reached the MPP and stop perturbing the operating point while P&O method allow the operating point oscillates around the MPP. Although, the IC method is more complicated compared to the P&O method, it can be easily implemented by the advancement of microcontrollers. However, this method requires the accuracy improvement at the steady state. [26]

To deal with this problem such has occurred for both P&O and IC method at the rapidly change of weather conditions, the variable-step size P&O and IC method [ 27] is proposed by increasing perturbation step size while the operating point is far from the MPP and decreasing step size on the other hand. However, it too difficult to relate the scaling factor of the perturbed step size to the non-linearity of the PV characteristic. The intelligence controller based MPPT is the solution and becomes very promising. FLC based MPPT and NFC based MPPT are two of them which are mentioned in the next section 3.2-3.5.

## 3.2 The Conventional Fuzzy Logic Control (FLC) based MPPT

Normally, most fuzzy logic control (FLC) based MPPT usually uses two inputs variable such as the error ($E$) and the change of the error ($CE$) at sampling time $k$ but with different variable representation. In this work, the slope of PV module's P-V curve, $S(k)$ ($\Delta P/\Delta V$) and the change of slope, $\Delta S(k)$ are used as the fuzzy input variable for $E$ and $CE$ respectively which are defined by eq. (13) and (14) respectively. $S(k)$ can easily determines the position of the operation point from the MPP which facilitates the increase or decrease of the duty cycle ratio while $\Delta S(k)$ can be used to determine the movement direction of the operating point or the magnitude of the change of duty cycle ratio to prevent fluctuations. The output of the FL is the difference of duty cycle ($\Delta D$) or the duty cycle ($D$) which are defined by eq. (15) and (16) respectively,

$$E(k) = \frac{P(k)-P(k-1)}{V(k)-V(k-1)} = \frac{V(k)I(k)-V(k-1)I(k-1)}{V(k)-V(k-1)} \quad (13)$$

$$CE(k) = E(k)-E(k-1) \quad (14)$$

$$\Delta D(k+1) = FGA(\{E(k), CE(k)\}) \quad (15)$$

$$D(k+1) = D(k) + \Delta D(k+1) \quad (16)$$

Typically, there are 3 steps of FLC including with fuzzification, inference, and defuzzification. Fuzzification step represents the different crisp variable by the predefined fuzzy subsets. In this work, slope of the $P$-$V$ curve and the change of this slope is selected as crisp variables. By our consideration, the crisp universe should be partitioned into five different subsets according to 5 regions of $P$-$V$ curve i.e. left-far from MPP, left-near to MPP, neighbor of MPP, right-near to MPP, and right-far from MPP that generate the total 25 subsets in fuzzy output universe. For partition of crisp universe, the popular Gaussian membership function has been chosen without any selection and representation in eq. (17),

$$\mu_i(x) = \exp\left[-\left(\frac{x-c_i}{\sigma_i}\right)^2\right] \quad (17).$$

Where $x$ is the crisp variable, $c$ and $\sigma$ are the mean and standard deviation of Gaussian function. The degree of membership function ($\mu$) ranging from 0 to 1 of each fuzzy input variable ($E$ and $CE$) are evaluated for the given crisp input. Then, the rules that contain IF-THEN statements which dictate the statement output are evaluated according to the compositional rule of interference. For example,

**Rule 1:** **if** $E$ is NB **and** $CE$ is PB **then** $D$ is PB
**Rule 2:** **if** $E$ is NB **and** $CE$ is NB **then** $D$ is $Z$

In this paper, we used Mamdani's interference typed Max-Min operation which is formulated as,

$$\mu_C(D) = \max\{\min\{\mu_A(E), \mu_B(CE)\}\} \quad (18)$$

where $\mu_A(E)$, $\mu_B(CE)$, and $\mu_C(\Delta D)$ are the membership value of the membership function of $E$,

*CE* and *D* respectively. After that, defuzzified this fuzzy output into a crisp output using the centre of gravity (COG) method,

$$\Delta D_{COG} = \sum_{j=1}^{n} \Delta D_j \mu_C(\Delta D_j) / \sum_{j=1}^{n} \mu_C(\Delta D_j) \quad (16)$$

where *n* is the number of fuzzy rule. In this work, the parameters of the membership function of the inputs and output are trial and error tuned and the interference rules have been experienced.

Generally, choosing a shape of MF, setting the interval or universe of discourse (UOD) and number of MF are very important since it is the great impact on the outcome of the FLC. The triangular membership function is simple and the suitable for the low cost microcontroller implementation while the bell-shape or Gaussian function performs well from the experience. However, if triangular produces the good results, more advance functions are not necessary. For the UOD, it is tuned by the trial and error by the tester. The design experiment results for MF selection between triangular and Gaussian MF with five MFs for input and output variable at the STC are shown in the section 4.2. To build up t he FLC based MPPT, a familiar experience of the user on traditional simplified the unknown system through the easy and understandable fuzzy rules. However, the number of fuzzy rules is usually excessive and the topology of the fuzzy sets is inappropriate by this human learning method. Since GA is the powerful searching method for optimal solutions in irregular and high-dimensional solution spaces. Another technique from using GA is adopted to generate the optimized fuzzy model are presented in the next sub-section.

### 3.3 FLC Designed by GA (FLC-GA) and the Optimized FLC-GA based MPPT

In [28], GA is used to search the parameters of the networks in an ANN based MPPT. In [29], FLC based MPPT optimized its parameters by using GA in the slow change of solar irradiance, the power fluctuation at the steady state is reduced in comparison with conventional fuzzy. In this work, GA is also used to optimize the parameters and control rules in FLC based MPPT for rapidly change of weather conditions both irradiance and temperature. However, due to the local minimum trap and slowly convergence to the global solution, GA may be accelerated by the initial solution from the solution of the previously FL control including membership function parameter and user experienced rules. The concept of the FLC based MPPT optimized by GA are shown by the block diagram in Fig. 6. The interfacing between PV module and FLC-GA is illustrated in Fig. 7.

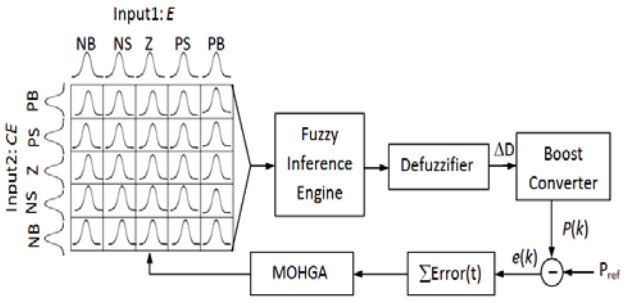


Figure 6. The block diagram of FLC with the parameter tuning by GA (FLC-GA) for MPPT algorithm.

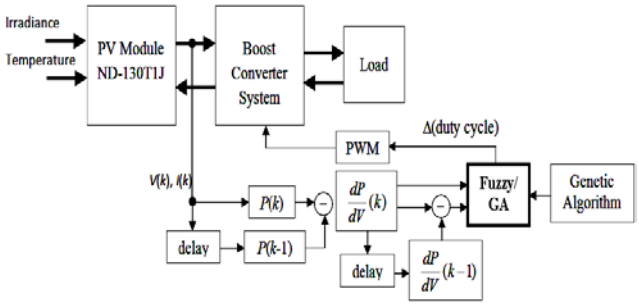


Figure 7. The FLC-GA based MPPT.

A brief outline of the FLC design for acquiring the best shape of MFs and selection best rule by using GA is illustrated in Fig. 8. The detailed stepwise procedures are described as follow;

Step1: The membership function for 2 inputs (*E*, Δ*E* or *CE*) and one output (*D* or Δ*D*) are constructed where each has 5 Gaussian membership functions as Negative Big (NB), Negative Small (NS), Zero (Z), Positive Small (PS), and Positive Big (PB). Each Gaussian function of each membership function has 2 adjusted parameters i.e. mean (*C*) and standard deviation ($\sigma$). Then, the total of 3×5×2= 30 parameters and 25 rules are adjusted and selected by GA in the evolution loop.

Step2: Initial population is generated by *M* chromosome. Each chromosome possesses vector entries with certain length of gene which is coded by binary code with the length of $N_{bit}$. The initial generation index (*Gen*) is then set to zero. In addition, the speed of GA procedure is accelerated by adding the extra chromosome which is tuned the parameter and designed the rule by human knowledge from the previous result.

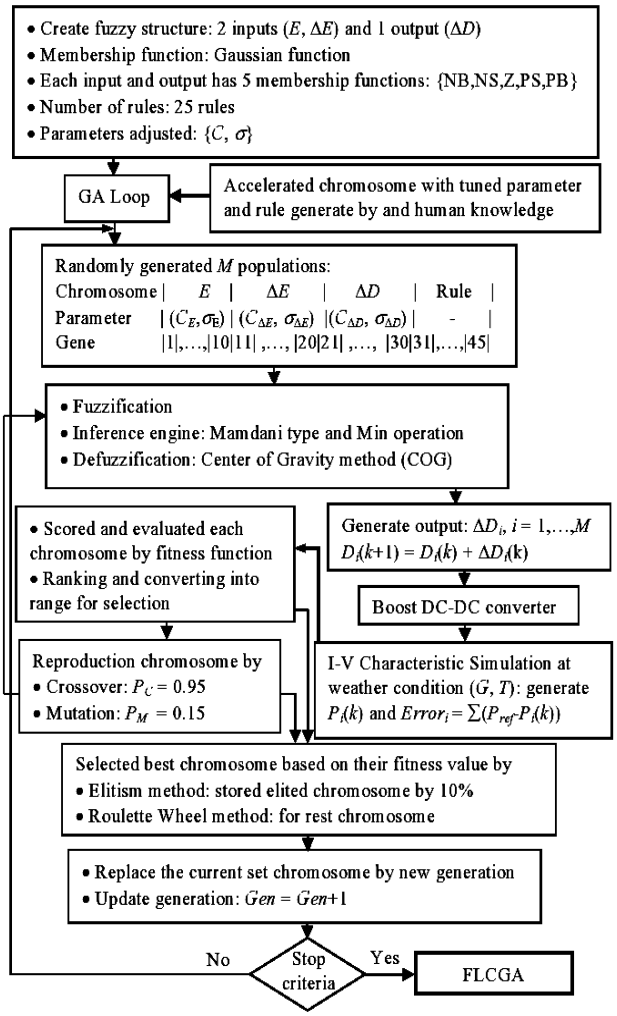


Figure 8. Flow chart of FLC-GA design procedure based MPPT.

Step3: The binary string of each gene is normalized within the range [$Q_{min}$, $Q_{max}$] by the linear mapping function as

$$gene(i) = \frac{(Q_{max,i} - Q_{min,i})}{2^{N_{Bit}} - 1} y(i) + Q_{min,i} \quad (17).$$

Here, $y(i)$ is real value converted from binary string of each gene. In this paper, the parameter $c$ and $\sigma$ of input $E$, and $\Delta E$, and output $\Delta D$ are normalized within the range [-20, 20], [0.1, 10], [-2, 2], [0.1, 1], [-1, 1], and [0.01, 0.5] respectively.

Step4: The output, $\Delta D$ of each chromosome is computed by the FLC based on MPPT. The PMW is then generated to switch the MOSFET switch of boost DC-DC converter. The output voltage at the current operating point moves to the new location according to the I-V characteristic of PV at the given weather condition. The difference of the power at time $k$ ($P_{k,i}$) and reference power ($P_{ref}$) of each chromosome is cumulatively sum up until the power difference does not change. The totally error, $Error_{k,i}$ is evaluated and scored for ranking chromosome as to their fitness function ($F$) as,

$$F_i = \frac{M_{POP}}{Err_i(C,W) + 1} \quad (18),$$

where

$$Err_i(C,W) = \sum_k (P_{k,i} - P_{ref})^2 \quad (19)$$

Thus, the higher scoring chromosome has the lower fitness values.

Step5: The parents based on their fitness value are chosen by two methods. First, the elitism method is used to retain the best chromosome that passes through the reproduction step at 10%. Second, the roulette wheel method is used to employ the remaining populations by assigning a higher probability of selection to individuals with higher fitness values.

Step6: Reproduction by crossover and mutation process with the probability $P_C$ and $P_M$ respectively options to determine how the GAs creates children for the next generation from the parents.

Step7: The new generation from step 6 is brought to replace the current population. Steps 2-6 are then repeated in the new generation until convergence is achieved. The algorithm stops if it meets the stopping criteria

### 3.4 Neuro-fuzzy Controller (NFC) based MPPT

The neuro-fuzzy system typically integrates the powerful learning of NNs and the high interpretability and computational efficiency by using reasoning rules of FL, thus this implies the most potential AI technique. In this work, neuro-fuzzy architecture like the ANFIS model performs as the controller-based MPPT directly generates the change of duty cycle based on the input including $E$ and $CE$ as defined in eq. (13) and (14). Unlike in researches [30]-[32], the MPP is previously generated from ANFIS model which uses the inputs from the weather conditions e.g. $G$ and $T$ then it was applied with another controllers to generate the duty cycle. More sensors are need twice from FLC which are not suitable for the small standalone PV system.

The structure of the ANFIS controller based on MPPT is shown in Fig. 9. The first order Sugeno or Takagi-Sugeno-Kang inference [33] was used for ANFIS which is different from Madani inference. While the Sugeno outputs are linearly a combination

of inputs instead of defuzzification method. Sugeno-type FIS has more advantages than Mamdani because it avoids the use of time consuming in defuzzification process since it is a more compact and computationally efficient representation. It also works well with optimization and adaptive techniques. Moreover it guarantees continuity of the output surface, and is well-suited to mathematical analysis. An example rule with the two fuzzy if-then rules can be expressed as:

**Rule 1**: **If** $E$ is PB **and** $CE$ is $Z$
**then** $\Delta D = p_1E + q_1CE + r_1$,
**Rule 2**: **If** $E$ is NB **and** $CE$ is PS
**then** $\Delta D = p_2E + q_2CE + r_2$,

where {NB, NS, Z, PS, PB} is fuzzy set in the antecedent and $\Delta D = f(E, CE)$ is a crisp function in the consequent part.

Generally, the rule which are obtained from the clustering or the grid partition based method are updated by NNs which uses back propagation learning method with gradient descent algorithm. Consequently, the premise parameters of the membership function ($C_i$, $\sigma_i$) are also optimized. While the consequently parameters: $p_i$, $q_i$, and $r_i$ are designed by least mean square (LMS) method. [34]. In this work, all of parameters are simultaneously selected by GA to avoid a local optimal trapping from the derivative method.

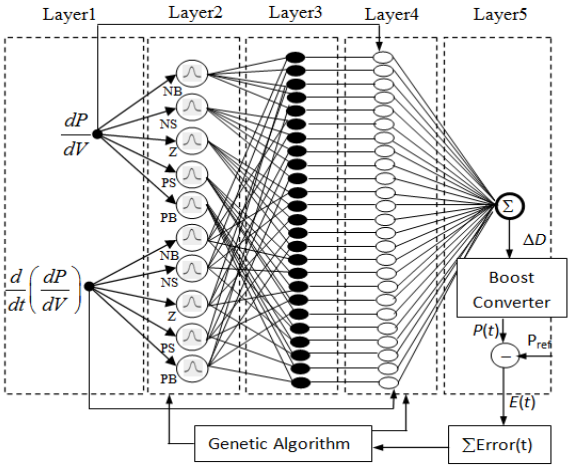


Figure 9. The block diagram of NFC (ANFIS) based MPPT.

The significant ANFIS based MPPT structure is detailed following:

Layer1: Each input node gives the crisp value to overall membership function in the fuzzy set.

Layer2: Each adaptive node generates the strength of membership function, $O_i^1 \in [0,1]$ for the input vectors. In this paper, the activation function is also Gaussian function which is represented in eq. (17).

Layer3: The total number of rule which is the product of membership function of set $E$ and $CE$ are 25 rules. Every node calculates the firing strength according to the rules via a multiplication,

$$O_i^2 = w_i = \mu_{1i}(E)\mu_{2i}(CE), \ i = 1,...,5 \quad (20)$$

Layer4: The strength of rule of each node in this layer has an averaging weighted as

$$O_i^3 = \overline{w}_i = w_i \Big/ \sum_{j=1}^{n} w_j \quad (21)$$

Layer5: Adaptive node $i$ in this layer computes the contribution of $i$-th rule towards the overall output, with the following node function, $O_i^4 = \overline{w}_i \Delta D_i$. Then overall output as the summation of contribution from each rule is finally computed as,

$$O_i^5 = \sum_{i=1}^{2} \overline{w}_i \Delta D_i \quad (22)$$

The trained parameters from 2×5×2 premise parameters and 5×5×3 consequent parameters are selected by GA with the chromosome representation as following;

| Chromosome | $E$ | $\Delta E$ | consequent parameter |
|---|---|---|---|
| Parameter | $(C_E, \sigma_E)$ | $(C_{\Delta E}, \sigma_{\Delta E})$ | $p,q,r$ |
| Gene | \|1\|, … ,\|10\|11\| | , … , \|20\|21\| | , … , \|95\| |

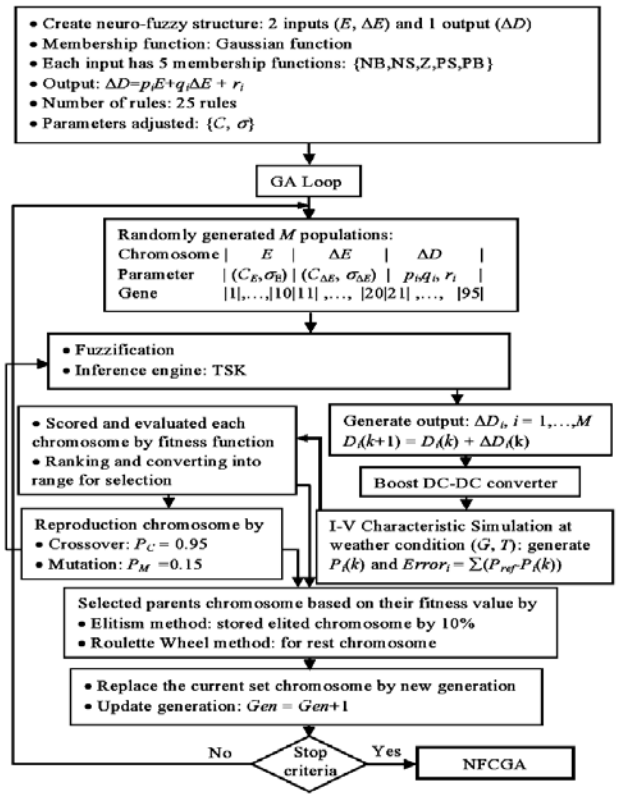


Figure 10. Flow chart of NFC-GA design procedure based MPPT.

The individual chromosome composed of three genes or variables including error ($E$), change of error ($CE$), and consequent parameter. The searching GA procedure for system parameter and the consequent parameter of each rule has the similar step in section 3.3 is not mentioned more and is shown in Fig. 10.

### 3.5 Optimized NFC-GA based MPPT

Basically, the rule node of ANFIS is formed by the linguistic fuzzy rule *if-then* model that is self-generated by the system. As the detail has shown in the previous section, the number of rule nodes is dependent on the $n$ number of inputs and $m_1$, $m_2$, …, $m_n$ number of linguistic fuzzy sets which are generated $m_1 \times m_2 \times \ldots \times m_n$ rules by default. In the estimation, the quality of parameter accuracy depends on e ffectiveness of these rules. However, all the self-generated rules do not contribute enough for an accurate improvement while increasing the computation time. In this work, the redundant rules are removed by GA while maintains the accuracy in acceptable. The ANFIS controller in the previous section is taken by rule reduction and simultaneously adjusting the parameter of the Gaussian function and consequent parameter of the significant rule. The structure of the rule reduced ANFIS is shown in Fig. 11. The significances of the proposed ANFIS structure including with the inference type are similarly with the previous one. GA is also used to optimize the system parameters simultaneously reduce the redundant rules.

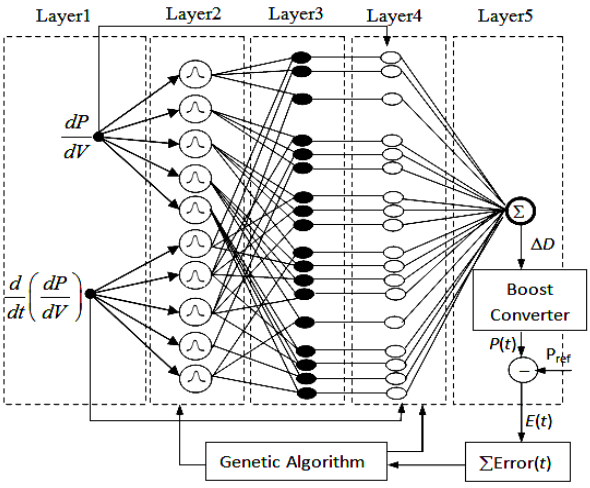


Figure 11. The block diagram of the optimized NFC-GA based MPPT.

In the GA design, the individual chromosome composes with genes which are represented for each parameter with the real value acceptable for rules. It served for the binary {0, 1} and shown in Fig. 4. In this work, 2 input $dP/dV$ and $d(dP/dV)/dt$ has each fuzzy set $m_1$ and $m_2$ respectively. They are presented by the Gaussian function with 2 adjusted parameters, $c$ and $\sigma$. The consequent parameters of each rule have 3 parameters, $p_i$, $q_i$, and $r_i$ according to first-order Sugeno fuzzy model. The $m_1 \times m_2$ rules set is randomly generated in binary code which is '0' means not consideration the accordingly rule while '1' means takes the rule into account for calculation.

| Chromosome | $dP/dV$ | $d(dP/dV)/dt$ | Consequence parameter | Rules |
|---|---|---|---|---|
| Parameter | $(C_G, \sigma_G)$ | $(C_T, \sigma_T)$ | $p_i, q_i, r_i$ | {1, 0} |
| Gene | $\lvert 1\rvert,\lvert 2\rvert,\ldots, \lvert 2m_1$ | $\lvert 1\rvert, \lvert 2\rvert,\ldots, \lvert 2m_2\rvert$ | $\lvert 1\rvert,\lvert 2\rvert,\lvert 3\rvert, \ldots, \lvert m_1 \times m_2 \times 3\rvert$ | $\lvert 1\rvert,\lvert 2\rvert, \ldots, \lvert m_1 \times m_2\rvert$ |

The searching GA procedure for system parameter, consequence parameter of each rule and for selecting significant rule has the similar step in section 3.3.

## 4. Results and Discussion

From the previous section, the various power control schemes based MPPT technique including with simple P&O, IC, conventional FLC, FLC-GA, optimized FLC-GA, NFC-GA, and optimized NFC-GA are already designed and tuned. In this section, the performance of their control for both transient and steady state with the various weather conditions are investigated and made the comparison among them. The weather conditions are set up in Fig. 10 by varying of the solar irradiance and temperature in the range 600-1,000 W/m$^2$ and 25-40°C respectively. At the initial condition, the weather is set up at STC and rapidly change to low irradiance and high temperature at $kT$ = 50. The rest weather condition is set to test the tracking performance. The cotrol results for individual scheme are described and discussed in next sub-section accordingly.

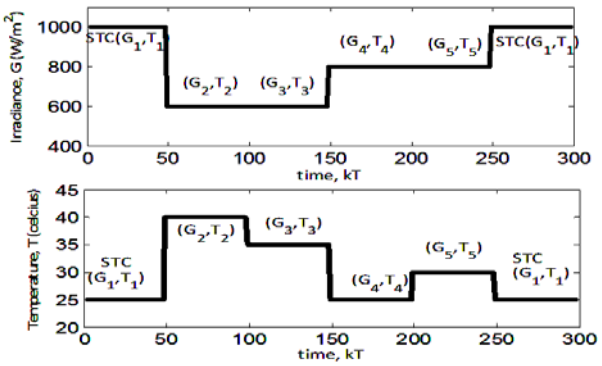


Figure 12. The various of solar irradiance and temperature conditions for the testing of controller based MPPT.

### 4.1 Power Control Effect from P&O and IC Method

The controlled results of the conventional P&O method through the set up of weather conditions represented in Fig. 10 are shown in Fig. 13. It has been seen that the convergence does not exitst for the small step size of $\Delta D$ with value of 0.001 while the drastical oscilation occurs for the high step size of $\Delta D$ with value of 0.05. The convergence at the steady state is achieved for the properly step size selection of $\Delta D$ with value of 0.02. However, the wide range of the risng time and oscilation still need more and more improvement. In the reference [23], the adaptive P&O fuzzy was proposed by replacing the comparing and switching step in P&O with fuzzy logic approach. The differential power ($\Delta P$) and differential voltage ($\Delta V$) are used as the input in this modified proposal. The rise time and oscilation are decreased by 60% and 80%, respectively. However, this proposed method has acchieved only in the case of slower change of the solar irradiance.

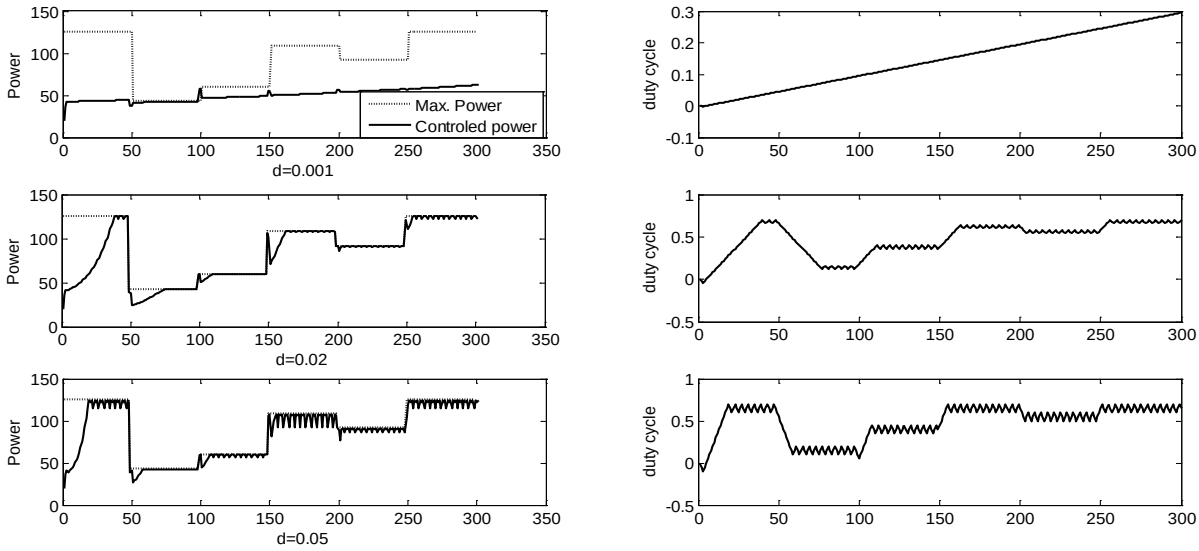


Figure 13. The controlled results from P&O controller with fixed duty cycle method based MPPT.

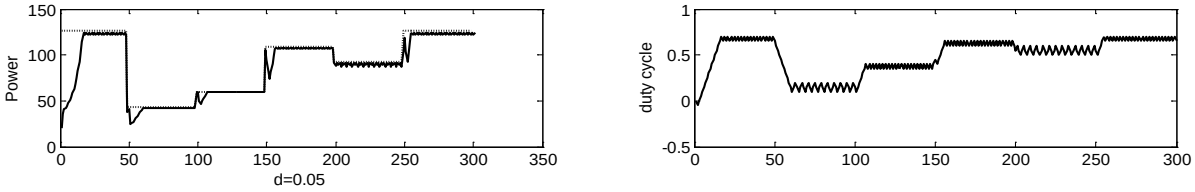


Figure 14. The control result of the IC controller based MPPT.

The simulation results under the same weather condition as represented in Fig. 12 by IC method is shown in Fig. 14 for the high perturbation step size equal to 0.05 for fast response. The rise time and oscillation are less in comparison with P&O method. However, the fluctuation and accuracy of MPP at the steady state needs more improvement. Further, requiring the complex and costly controlled circuits of this method is the disadvantages with respect to P&O method.

The tracking time performance for both P&O and IC methods at the fastest change weather conditions are quite well since they take a low rise time but the accuracy and fluctuation becomes clearly worse at the steady state. To overcome such the problems, our proposed FLC and NFC are implemented to assist the conventional controllers to obtain the MPP faster and more stable PV output power.

### 4.2 Power Control Effect of the Conventional FLC, FLC-GA and Optimized FLC-GA

The results of the MFs of the inputs and output in both triangle and the Gaussian MF from the design in previous section are shown in Fig. 15 and Fig. 16 respectively. It was noticed that the membership functions of the duty cycle was not distributed evenly along the universe of discourse (UOD). They were designed for more dense in the range [-0.2, 0.2] which was a sensitively worked zone to achieve near the MPP.

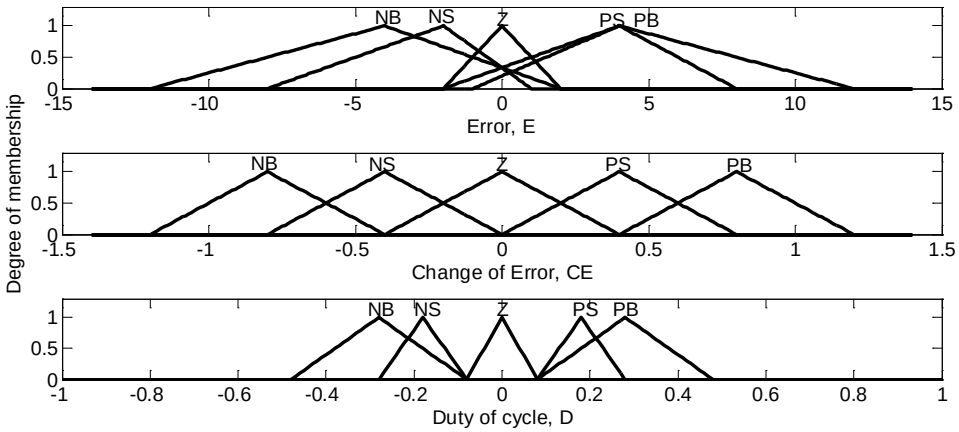


Figure 15. The user designed for the triangular MFs of the input *E* and *CE* and the output Δ*D*.

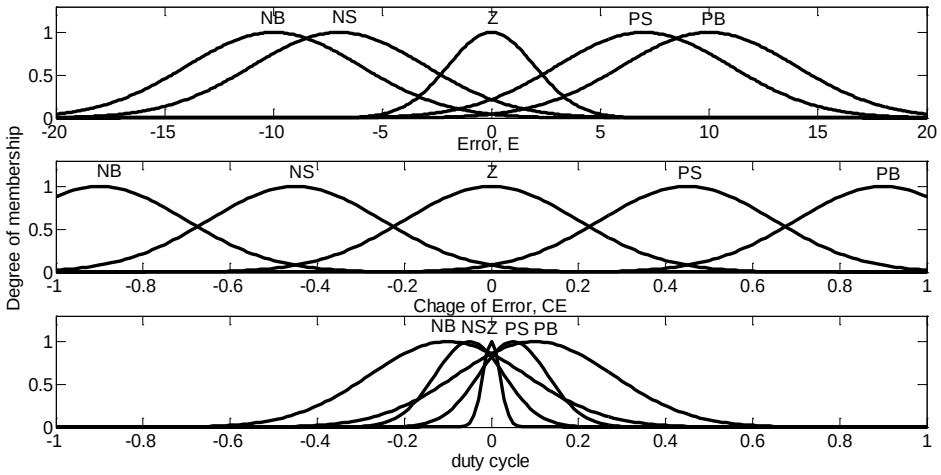


Figure 16. The user designed for Gaussian MFs of the input *E* and *CE* and the output Δ*D*.

The fuzzy rules are designed here to incorporate the following keeping in view the overall control performance

- For the case of the slope of *P-V* curve or *S*(*k*) is NB and Δ*S*(*k*) is Z means the operation point of the PV module is located at the right side and near the MPP, then the duty cycle ratio needs to increase following eq. (10) for decreasing the input impedance in order to shift the operating point to the MPP at the left side. The controlled output is then set to PS to suppress the change of magnitude of the duty ratio in the opposite direction. However, when Δ*S*(*k*) is NB or NS which means the direction towards to the right side then the output control would be set to Z in order to prevent the operating point shift to the left side of the MPP and oscillation. For the case of Δ*S*(*k*) is PS or PB, the output control would be set as NS or NB for increasing the duty cycle ratio in order to shift the operating point to the left according to the movement direction. When *S*(*k*) is NS and Δ*S*(*k*) is either negative or zero or positive, the duty cycle ratio under this condition was set in the similar way.

- For the case of *S*(*k*) is PB and Δ*S*(*k*) is Z, this means that the operating point of the PV module is located at the left side and near of the MPP, then the duty cycle ratio needs to be decrease following eq. (10) for increasing the input impedance in order to shift the operating point to the MPP at the right side. When Δ*S*(*k*) is also PB or PS, the controller may generate the wrong outputs owing the reason similar to the above mentioned then the controlled output would be set as Z. When Δ*S*(*k*) is NB or NS, the operating point would be set to increase the duty cycle ratio. Then the output control would use PB or PS respectively. When *S*(*k*) is PS and Δ*S*(*k*) is either negative or zero or positive, the duty cycle ratio under this condition was set in the similar way.

- For the case of $S(k)$ is Z and $\Delta S(k)$ is Z, the controlled output would be set Z. When $\Delta S(k)$ is NB or NS the controlled output would be set to PB or PS respectively and when $\Delta S(k)$ is PB or PS the controlled output would be set to NB or NS respectively.

Taking this reason into consideration, the fuzzy rules are derived and the corresponding rule based on 25 r ules for both triangular and Gaussian MF are given in Table 1.

Table 1 Fuzzy rule base designed by user experience of FL based MPPT

| | | ***E*** | | | | |
|---|---|---|---|---|---|---|
| | | **NB** | **NS** | **Z** | **PS** | **PB** |
| ***CE*** | **NB** | Z | Z | PB | PB | PB |
| | **NS** | Z | Z | PS | PS | PS |
| | **Z** | PS | Z | Z | Z | NS |
| | **PS** | NS | NS | NS | Z | Z |
| | **PB** | NB | NB | NB | Z | Z |
| | | Right side of MPP | | Near MPP | Left side of MPP | |

The controlled results of the conventional FLC with using triangular MFs where the inference rule base is obtained from the user experienced design are shown in Fig. 18 for the various weather conditions represented in Fig.12. The effect of the power control by the user designed FLC using triangular MF for the input and output variable with the same weather conditions test used in P&O and IC method are shown in Fig. 12. It is seen that at the lower irradiance and high temperature (at $kT$=50) the tracking performance is failed from achieving the MPP target.

Comparing with the user designed FLC results using the triangular MFs and Gaussian MFs in Fig. 17 and 18, it can be seen that the tracking performance of the latter case is better than the former one. At the low irradiance and high temperature condition ($kT$=50), the tracking had successfully reaches near a steady MPP at about $kT$ equal to 85. In addition, the accuracy on the MPP and the fluctuation at the steady state are minor improvement compared with the conventional methods. This is due to the ability of automatically reducing perturbed voltage after the MPP is identified unlike to the conventional method that is still performing the same size of the perturbed voltage. However, the high rise time at the transient state and the oscillation and accuracy at the steady state need to consequently develop as seen obviously in Fig. 16(C).

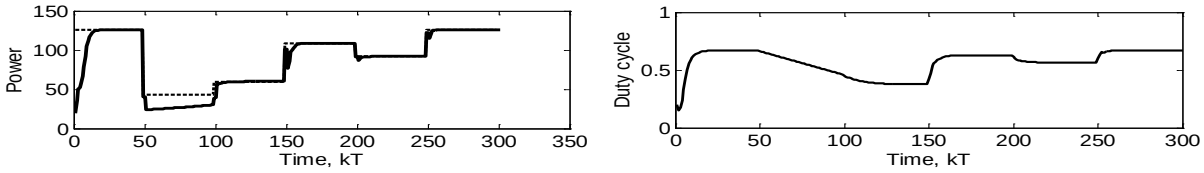


Figure 17 The control results of the conventional FLC for the triangular MF based MPPT.

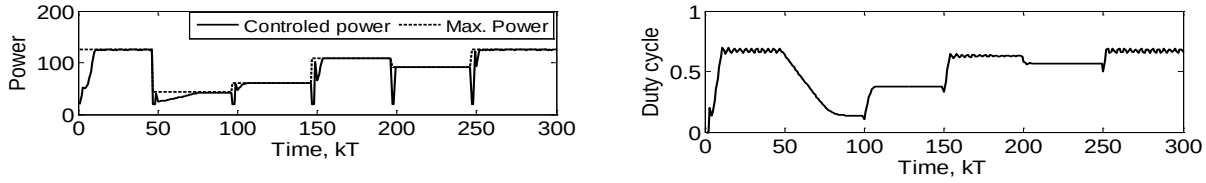


(a) the power tracking for the fast change of weather conditions (b) variation of duty cycle ratio

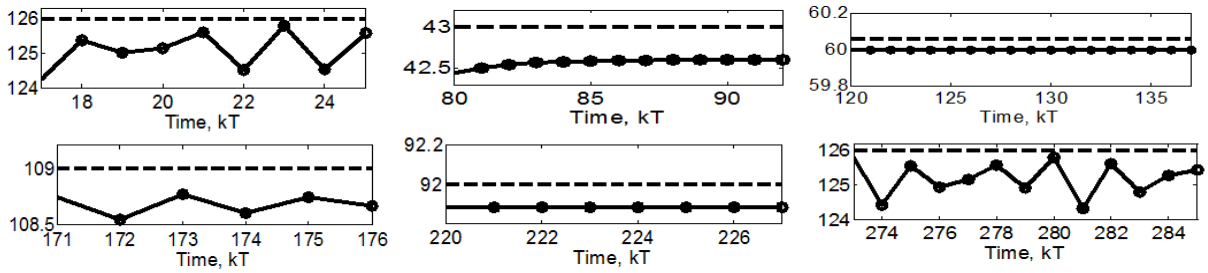


(c) the fine difference between power point produced from the controller and the MPP at each weather condition

Figure 18. The control results of the conventional FLC by using the Guassian MFs based MPPT.

To achieve more improvement controlled results, the shape of Gaussian MFs and the rules are designed and selected by MOHGA following the detailed procedure in section 3.2. After all computations are performed by using MATLAB program, the best shape of five Gaussian MFs of the inputs and output are shown in Fig. 19 and the selected fuzzy rules are shown in Table 2.

Table 2 The designed fuzzy rule base of FLC-GA.

| CE \ E | **NB** | **NS** | **Z** | **PS** | **PB** |
|---|---|---|---|---|---|
| **NB** | Z | Z | PB | PB | PB |
| **NS** | Z | PS | PS | PS | PB |
| **Z** | PS | NS | Z | Z | Z |
| **PS** | NS | NB | NS | NS | Z |
| **PB** | NB | NB | NS | NS | Z |

From Table 2, t he rule base has change differently from the previously design by the user. The fuzzy set Z of the controlled output is replaced by the fuzzy set NS and PS which is corresponding with the same location of Z, PS, and NS of the output MF in Fig. 19. The UOD of the output Gaussian MFs are still dense in the range of [-0.2, 0.2] but a little shifting to the left hand side of the zero in spite of symmetry around the zero. It showed that more reduced step size of perturbed voltage was desired to achieve the MPP.

The control results of our proposed FLC-GA under the fast change of weather conditions represented in Fig. 12 are shown in Fig. 20. By the comparison, our proposed FLC-GA performs fast time response and less overshoot at the transient state and more stable and high accuracy at the steady state than the user designed FLC, the conventional P&O, and IC method. However, it is observed that the rise time takes a n umber of the time steps at the rapidly change condition i.e. especially at the low irradiance and high temperature at $kT$ =50 and 150. The overshoot has firstly appeared through this control method. To improve the transient response performance of the FLC-GA, and further for more accuracy at the steady state the parameters and the control rule should be simultaneously optimized by GA. The redundant rules are eliminated through this method which makes the controller more efficiency and effective.

For the optimized FLC, the genes for rule number parameter in chromosome are modified by randomly adding '0s' for reducing the redundant rule simultaneously optimized the parameter of membership function. The best shape of five membership functions of inputs and output are shown in Fig. 21 and the optimized fuzzy rule base are shown in Table 3. The fuzzy rule is reduced to remain 21 r ules from 25 r ules. Now, the shape of MFs and UOD are differently changed with the difference controlled rule comparing the previous results that cannot explicitly explain this mechanism. The control performance of another version of FLC-GA which was reduced the controlled rule are shown in Fig. 22 under the same weather conditions represented in Fig. 12.

Table 3 The optimized fuzzy rule base of F-GA controller designed by GA method.

| *CE* \ *E* | NB | NS | Z | PS | PB |
|---|---|---|---|---|---|
| NB | - | Z | PB | PB | Z |
| NS | Z | PS | - | PS | PS |
| Z | NB | - | PS | PS | NB |
| PS | PB | PB | NS | PB | NB |
| PB | PB | NB | - | PS | NB |

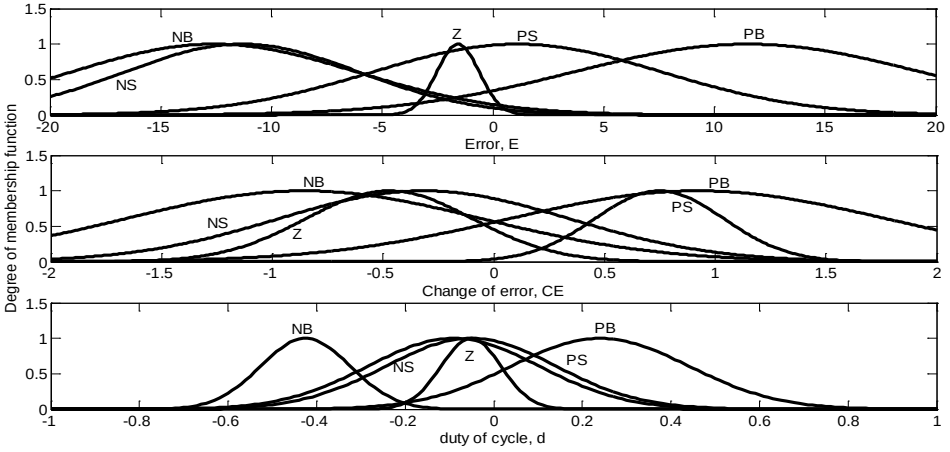


Figure 19. The shape of Gaussian MFs of the input variable *E* and *CE* and

the output variable *D* which are selected by MOHGA for FLC-GA based MPPT.

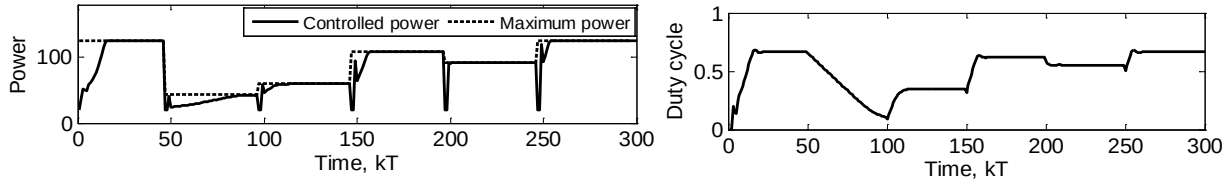


(a) the power tracking for the fast change of weather conditions (b) variation of duty cycle ratio

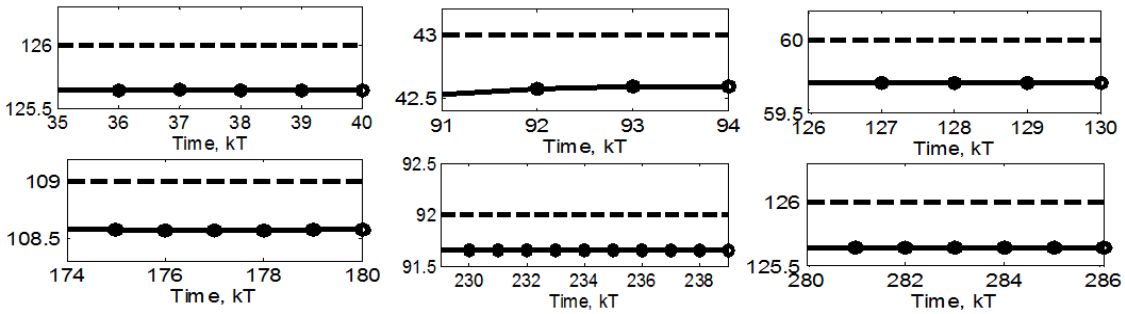


(c) the fine difference between power point produced from the controller and the MPP at each weather condition

Figure 20. The control results of the proposed FLC-GA controller based MPPT.

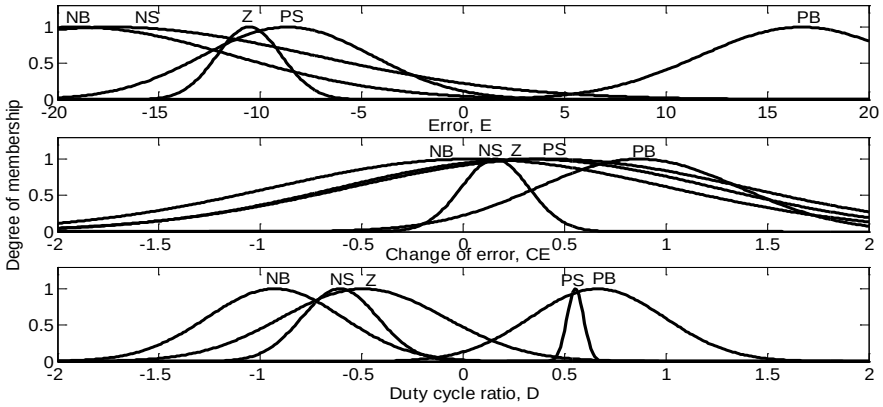


Figure 21. The best shape of MFs and their parameters which are searched by GA method for the input variable *E* and *CE* and the output variable Δ*D* of the optimized FLC-GA based MPPT.

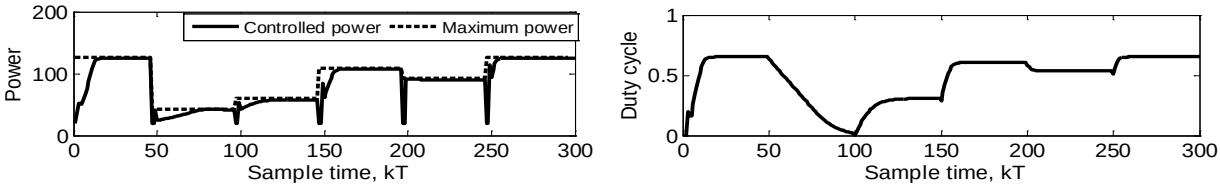


(a) the power tracking for the fast change of weather conditions (b) variation of duty cycle ratio

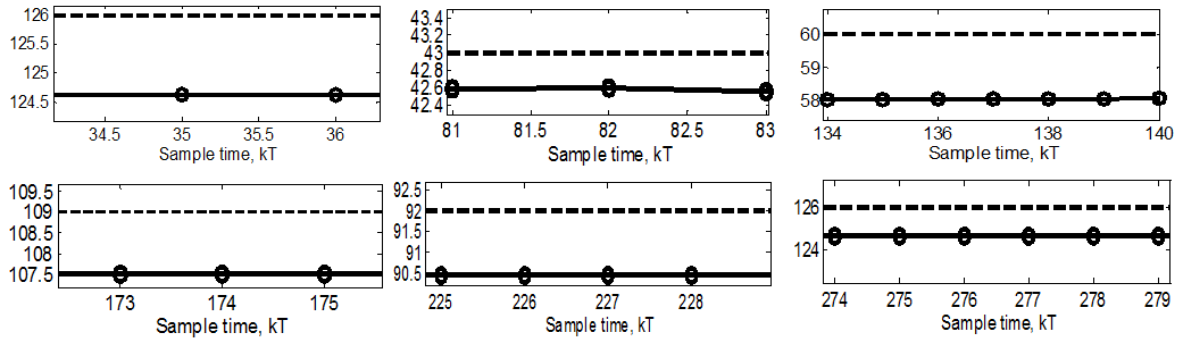


(c) the fine difference between power point produced from the controller and the MPP at each weather condition

Figure 22. The control results of the optimized FLC-GA based MPPT.

It can be seen that the controlled results by the optimized FLC-GA at the rapidly change condition (i.e especially *kT*= 50 and 150) has the rise time better than the conventional FLC and FLC-GA with full rule by approximately 22.5% and 25% respectively. The average accuracy at steady state is less than the FLC-GA about 5.14% but higher than the conventional FLC about 8.56% by approximation. However, the accuracy at steady state for the rapidly change condition is quite worse and less than the FLC-GA and conventional FLC about 71.80% and 77.67% by approximation.

To improve the accuracy together preserve the fast transient response especially for the case of very low irradiance and high temperature, another proposed controller by using NFC is investigated the next sub-section in order to challenge the trade-off between fast transient response and accuracy at the steady state.

### 4.3 Power Control Effect of NFC-GA and Optimized NFC-GA

After the designed NFC by GA procedure in section 3.4 , the best shape of MFs of the inputs *E* and *CE* are shown in Fig. 23 and all 20 premise parameters and 75 consequent parameters are also obtained but are not shown here.

The controlled results by our proposed NFC-GA are shown in Fig. 24 where the system parameters were designed by GA under the weather conditions represented in Fig. 12. By the comparison, our proposed NFC-GA performs the rise time for the rapidly change weather condition less than the optimized FLC-GA, the user designed FLC, and FLC-GA respectively. The accuracy of MPP at the steady state by this method is more accurate over the other controllers which are mentioned above. However, the overshoot has severely occurred at the transient state.

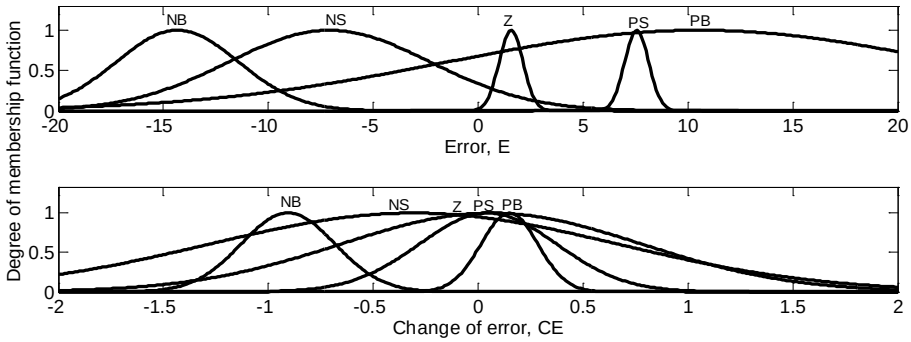


Figure 21 The best shape of MFs and their parameters which are searched by GA method for the input variable *E* and *CE* of the NFC-GA based MPPT.

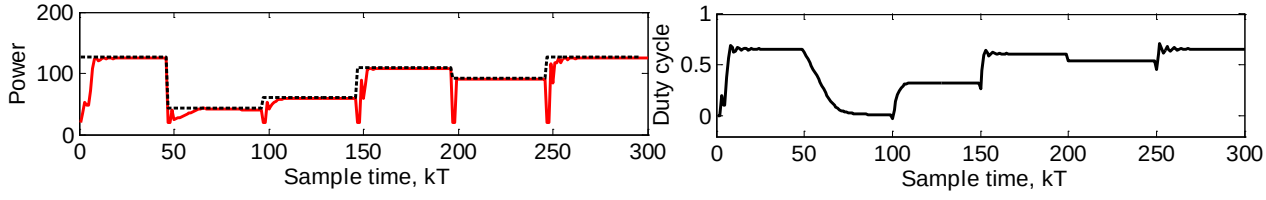


(a) the power tracking for the fast change of weather conditions (b) variation of duty cycle ratio

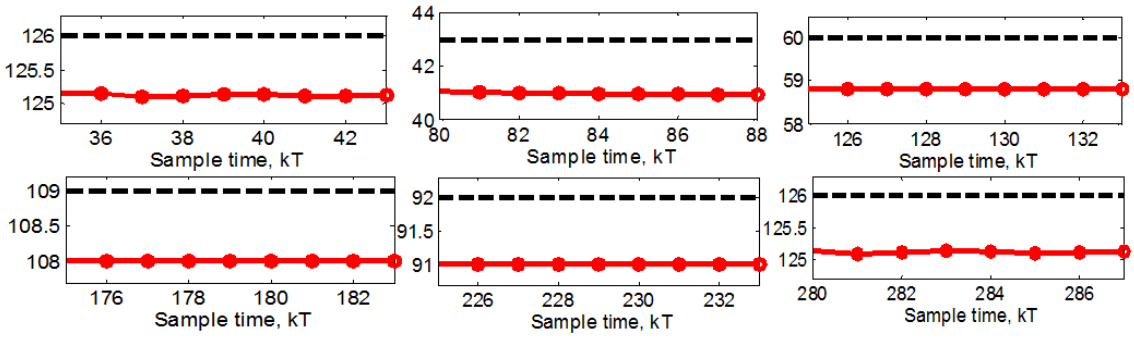


(c) the fine difference between power point produced from the controller and the MPP at each weather condition

Figure 22 The control results of NFC-GA based MPPT.

After the design of optimized NFC by GA procedure in section 3.5, the best shape of MFs of the inputs *E* and *CE* are shown in Fig. 23. The number of rule is reduced by 10 r ules. The remaining parameter of this ANFIS model is totally 65 parameters which are reduced by 30 parameters from the original ANFIS model. All parameters are also obtained but not shown here. The controlled results from this optimized NFC-GA are shown in Fig. 24. The high complex structure of NFC-GA including many system parameters which may lead ineffective controller is optimized through the description in section 3.5. The controlled results by applying optimized NFC-GA are shown in Fig. 24. It is found that the rise time from the optimized NFC-GA is lower than the NFC-GA by 15% but more oscilation and overshoot in the transient state. However the accuracy at stady state is not difference where the optimized NFC-GA has the error less than the NFC-GA by about 2.14%. It can be seen that the reduced rule strategy both FLC and NFC has successful approve the time response and dominated than the improvement of accuracy.

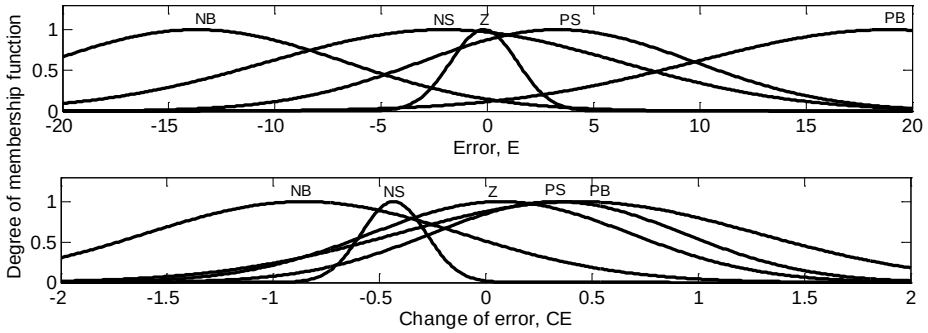


Figure 23. The best shape of MFs which are searched by MOHGA for the input variable *E* and *CE* of the optimized NFC-GA based MPPT.

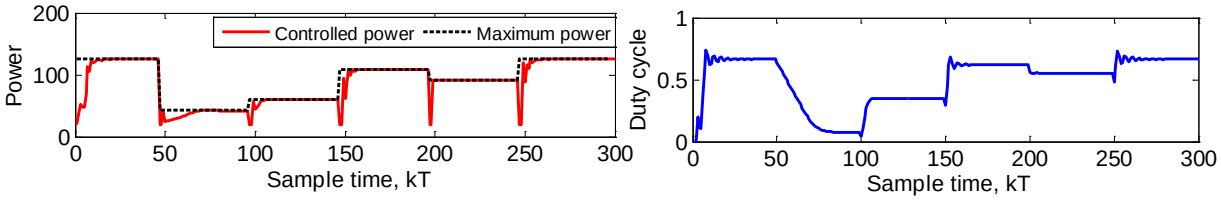


(a) the power tracking for the fast change of weather conditions (b) variation of duty cycle ratio

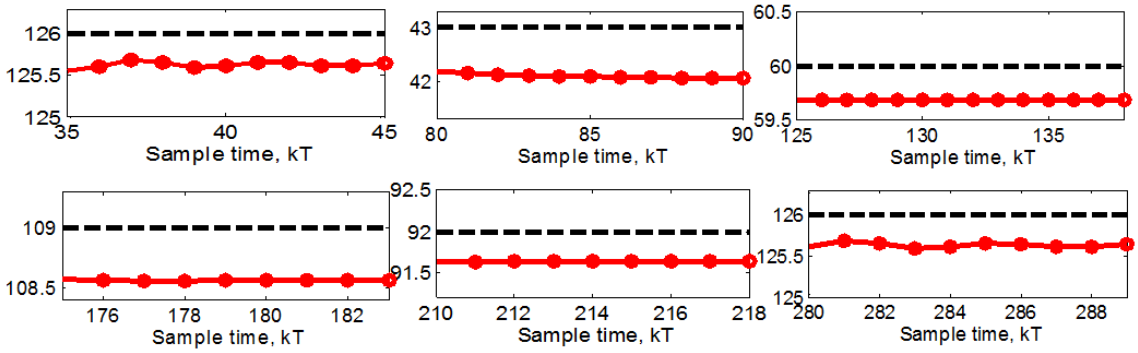


(c) the fine difference between power point produced from the controller and the MPP at each weather condition

Figure 24. The control results of the optimized NFC-GA based MPPT.

## 4.4 Comparison Performance of the Controllers

From the overall results of the performance at the transient and steady state from all controllers obtained from the simulated testing, are comparatively shown in Table 4 which has its own advantages and disadvantages with respect of each controller. The FLC-GA performs the best accuracy with closely tracking nearly the MPP better than the optimized NFC-GA, NFC-GA, optimized FLC, the conventional FLC, IC and P&O by about 1.22%,

4.95%, 5.14%, 5.58%, 6.10%, and 6.32% respectively. For the rise time, the optimized NFC-GA performs the fast tracking to the MPP better than the NFC-GA, optimized FLC-GA, conventional FLC, FLC-GA, P&O, and IC by about 3.76%, 7.50%, 8.75%, 42.27%, 67.05%, and 72.50% respectively.

However, the optimized NFC-GA based ANFIS structure is considered to perform the best result by trade-off between the transient and steady state except for the existing of the overshoot is only its disadvantage.

Table 4 Comparison performance of the controllers based MPPT in the case of fast change weather conditions

| Controller | Transient state | | Steady state | |
|---|---|---|---|---|
| | Overshoot | Rise time | Oscillate | Accuracy |
| Conventional P&O | None | Medium | High | Low |
| Conventional IC | None | Low | High | Low |
| User design FLC | None | Medium | Medium | Medium |
| FLC-GA | Low | High | None | Very High |
| Optimized FLC-GA | Low | Low | None | Medium |
| NFC-GA (ANFIS) | Medium | Low | None | High |
| Optimized NFC-GA | High | Very low | None | High |

# 5 Conclusion

This paper implements the fuzzy logic controller (FLC) and neuro-fuzzy controller (NFC) or ANFIS structure based on maximum power point tracking (MPPT) for a solar photovoltaic module. The proposed FLC and NFC are intentionally implemented to improve the controlled performance of P&O method, IC method and the conventional FLC controller. The design and selection of the system parameters including to the controlled rules of the FLC and NFC are properly trained and tuned by MOHGA and denoted FLC-GA and NFC-GA respectively. However, the high complex of these proposed controllers may lead the over-fitting and miss matched the desire MPP. The optimized rules and simultaneous parameter reducing of FLC and NFC by MOHGA are assumed to replace the former FLC-GA and NFC-GA and denoted optimized FLC-GA and optimized NFC-GA. In order to test the performance of the all proposed controllers, the simulation and testing results were performed on Matlab/Simulink program before the practical implementation. In our experiment, a polycrystalline silicon commercial (SHARP type ND-130T1J) with 36 cells in connected series is adopted to study. The PV module parameters of the single diode equivalent circuit model are extracted by using the NNs estimated model together with simple GA and the parameter translation functions in order to generate the *I-V* and *P-V* characteristic under the various weather conditions of both irradiance and temperature. This solar PV module is connected to a resistive load with interfacing by the DC-DC boost converter. The directly measured current and voltage from the panel are computed the slope of *P-V* curve and its change to use as the input for all controllers while the duty cycle is generated as the controlled output. The controlled performance at the transient and steady state covers the maximum overshoot, the rise time, the stability and the accuracy. The optimized NFC-GA clearly performs the best performance over the rest controllers by the trade off between the fast time response and high stabilized accurate tracking except the disadvantage for the exiting overshoot.

In the future, the NFC may be utilized the weather condition as the input to estimate the MPP and perform FLC-GA or NFC-GA for improving the control performance. Furthermore, the other optimization techniques such as the particle swarm optimization (PSO), artificial bee colony (ABC), etc. are used to optimize the FLC and NFC for alternate searching strategy. Moreover, the weather condition may be taken the fading effect for consideration to challenge the controller performance.

*References:*

[1] B.K. Bose, "Global Warming Energy: Environmental pollution and the impact of power electronics," *IEEE Industrial Electronics Magnzine*, 2010, pp. 1-17.

[2] International Energy Agency (IEA), "**Southeast Asia energy outlook 2015**," World Energy Outlook Special Report, 2015. Available online at:www.iea.org. (Last accessed on January, 2016)

[3] C. L. Hou, "Appliction of adaptive of solar cell battery charger," *IEEE DRPT*, 2004.

[4] A. Chouder, F. Guijoan, and S. silvestre, "Simulation of fuzzy-based MPP tracker and performance comparison with perturb & observe method," *Revue des Energies Renouvelables*, Vol. 11, No. 4, 2008, pp. 577-586.

[5] V. Salas, E. Olias, A. Barrado and A. Lazaro, "Review of the maximum power point tracking algoithms for stand-alone photovoltaic systems," *Solar Energty Material & Solar Cells*, Vol. 90, 2006, pp. 1555-1578.

[6] D.P. Hohm and M.E. Ropp, "Comparative study of maximum power point tracking algorithms," *Progress in Photovoltaics: Research and Applications*, 2002, pp. 47-62.

[7] R. Faranda and S. Leva, "Energy comparison of MPPT techniques for PV systems," *WSEAS Trans. On Power Systems*, vol.3, issue 6, 2008, pp. 446-456.

[8] C. Rodriguez and G.A.J. Amartatunga, "Analysis solution to the photovoltaic maximum power point tracking problem," *IEEE Trans. On Circuits and Systems*, vol. 54, no. 9, 2007, pp. 2054-2060.

[9] A. Mellit, S. A. Kalogirou, L. Hontoria and S. Shaari, "Artificial intelligence techniques for sizing photovoltaic sytem: A Review," *Renewable and Sustainable Energy Reviews*, vol. 13, 2009, pp.406-419.

[10] S. Haykin, **Neural network-A comprehensive foundation**, 2nd edition, New York Practice Hall Inc., 1999.

[11] T. Hiyama and K. Kitabayashi, "Neural network based estimation of maximum power point generation from PV module using enviromental information," *IEEE Trans. On Energy Conv*., vol. 12, no. 3, 1997, pp. 241-247.

[12] A. AI-Amoudi and L. Zhang, "Application of Radial Basis Function networks for solar-array modelling and maximum power-point prediction," *IEE Proc. Generation, Transmission and Distribution*, vol. 147, no. 5, 2000, pp. 310-316.

[13] S. Premrudeepreechachan and N. Patanapirom, "Solar-array modeling and maximum power point tracking using neural networks," *IEEE Bologna Power Tech Conf*., 2003.

[14] G. Chen and T.T Pham, **Introduction to fuzzy sets, fuzzy logic, and fuzzy control systems**, CRC Press, 2000.

[15] M.S. Kaisar, A. Anwer, S.K. Aditya, and R.K. Mazumder, "Design and simulation of fuzzy based MPPT," *Renewable Energy Prospect and Progress*, 2005, pp. 19-21.

[16] T.L. Kottas, Y.S. Boutalis and A.D. Karlis, "New maximum power point tracker for PV array using Fuzzy controller in closed cooperation with fuzzy cognitive network," *IEEE Trans. On Energy Conv*., vol. 21, no. 3, 2006.

[17] A.M.S Aldobhani and R. John, "Maximum power point tracking of PV system using ANFIS prediction and fuzzy logic tracking," *Proc. Int. Multiconf. Of Engineeris and Computer Scientists IMECS*, 2008.

[18] A. Iqbal, H. Abu-Rub, and S.M. Ahmed, "Adaptive neuro-fuzzy inference system based maximum power point tracking of a solar pv module," *IEEE Int. Energy Conf*., 2010, pp.51-56.

[19] T. Shanthi, and A.S. Vanmukhil, "ANFIS controller based MPPT control of photovoltaic generation system," *Int. J. of Comp. Applications*, 2013, pp.23-29.

[20] B. Tarek, D. Said, and M.E.H. Benbouzid, "Maximum power point tracking control for photovoltaic system using adaptive neuro-fuzzy, ANFIS," *IEEE Conf. and Exhibition on Ecological Vehicles and Renewabel Energies* (EVER), 2013.

[21] G.Walker, "Evaluating MPPT converter topologies using a MATLAB PV model," *J. Elect. Electron. Eng. Australia*, 21(2001)49-56.

[22] M.A. De Blas, J.L. Torres, E. Prieto, A. Garcia, "Selecting a suitable model for characterizing photovoltaic devices," *Renewable Energy*, 25(2002)371-380.

[23] M.A.A. Mohd Zinuri, M. A. Mohd Radzi, and A. Chesoh, "Adaptive P&O-Fuzzy control MPPT for PV boost DC-DC converter," IEEE Int. Conf. on Power and Energy (PECON), 2012, pp. 524-529.

[24] S.R. Chafle and U.B. Vaidya, "Incremental Conductance MPPT Technique for PV system," Int. J. of Advanced Research in Elect. And Instr. Eng., vol. 2, issue 6, 2013, pp. 2719-2726.

[25] F. Liu, S. Duan, F. Liu, B. Liu and Y. Kan, "A variable step size INC MPPT method for PV system," IEEE Trans. Ind. Electron., vol. 55, no. 7, 2008, pp. 2622-2628.

[26] Saoud, M.S. Abbassi, H.A., Kermiche, S. Ouada, M. Improved incremental conductance method for maximum power point tracking using cuk converter. WSEAS Trans. On Power Sys. 3(8)(2013)124-133.
[27] Jiang, Y. Qahong, J.A.A. Haskew, T.A. Adaptive step size with adaptive-perturbation-frequency digital MPPT controller for a single-sensor photovoltaic solar system. IEEE Trans. Power Electron. 2013,28, 3195-2305.
[28] R. Ramaprabha, and B.L. Mathur, "Intelligent controller based maximum power point tracking for solar PV system," Int. J. of Comp. Appl., vol. 12, no. 10, 2011, pp 37-41.
[29] A. Rezaei, and A. Gholamian, "Optimization of new fuzzy logic controller by genetic algorithm for maximum power point tracking in photovoltaic system," ISESCO J. of Sci. and Tech., vol. 9, 2013, pp. 9-16.
[30] Iqbal, A., Abu-Rb, H. and Ahmed, Sk.M. Adaptive Neuro-fuzzy Inference System based Maximum Power Point Tracking of a Solar PV Module. IEEE Int. Energy Conf. (2010)51-56.
[31] Ahmed, B.H. Abdennour, A. and Mashaly, H. An Accurate ANFIS-based MPPT for Solar PV System. Int. J. of Adv. Comp. R. 4(2)(2014)2249-7277.
[32] Shanthi, T. and Vanmukil, A.S. ANFIS Controller based MPPT Control of Photovoltaic Generation System. Int. J. of Comp. Appl. (2013)23-29.
[33] L. Wang, et al., "Wind power systems, green energy and technology," Springer-Verlag Berlin Heidelberg, 2010, pp. 255-295.
[34] M. Balaji Naik, and P. Sujatha, "Adaptive fuzzy & neuro-fuzzy inference controller based MPPT for photovoltaic systems," Int. Research J. of Eng. and Tech. (IRJET), vol. 2, issue 8, 2015, pp. 693-701.